Skeletal Radiol (2015) 44:1709–1725
DOI 10.1007/s00256-015-2182-9

REVIEW ARTICLE

Advanced imaging of the scapholunate ligamentous complex

Maryam Shahabpour[1] · Barbara Staelens[2] · Luc Van Overstraeten[3] · Michel De Maeseneer[1] · Cedric Boulet[1] · Johan De Mey[1] · Thierry Scheerlinck[2]

Received: 1 February 2015 / Revised: 21 May 2015 / Accepted: 25 May 2015 / Published online: 30 July 2015

Abstract The scapholunate joint is one of the most involved in wrist injuries. Its stability depends on primary and secondary stabilisers forming together the scapholunate complex. This ligamentous complex is often evaluated by wrist arthroscopy. To avoid surgery as diagnostic procedure, optimization of MR imaging parameters as use of three-dimensional (3D) sequences with very thin slices and high spatial resolution, is needed to detect lesions of the intrinsic and extrinsic ligaments of the scapholunate complex. The paper reviews the literature on imaging of radial-sided carpal ligaments with advanced computed tomographic arthrography (CTA) and magnetic resonance arthrography (MRA) to evaluate the scapholunate complex. Anatomy and pathology of the ligamentous complex are described and illustrated with CTA, MRA and corresponding arthroscopy. Sprains, mid-substance tears, avulsions and fibrous infiltrations of carpal ligaments could be identified on CTA and MRA images using 3D fat-saturated PD and 3D DESS (dual echo with steady-state precession) sequences with 0.5-mm-thick slices. Imaging signs of scapholunate complex pathology include: discontinuity, nonvisualization, changes in signal intensity, contrast extravasation (MRA), contour irregularity and waviness and periligamentous infiltration by edema, granulation tissue or fibrosis. Based on this preliminary experience, we believe that 3 T MRA using 3D sequences with 0.5-mm-thick slices and multiplanar reconstructions is capable to evaluate the scapholunate complex and could help to reduce the number of diagnostic arthroscopies.

Keywords Scapholunate ligament complex · Imaging · MR arthrography · CT arthrography · Wrist arthroscopy

✉ Maryam Shahabpour
maryam.shahabpour@uzbrussel.be

Barbara Staelens
barbarastaelens@hotmail.com

Luc Van Overstraeten
l.v.o@skynet.be

Michel De Maeseneer
michel.demaeseneer@uzbrussel.be

Cedric Boulet
cedric.boulet@uzbrussel.be

Johan De Mey
johan.demey@uzbrussel.be

Thierry Scheerlinck
thierry.scheerlinck@uzbrussel.be

[1] Department of Radiology, Universitair Ziekenhuis Brussel (UZ Brussel), Laarbeeklaan 101, 1090 Brussels, Belgium

[2] Department of Orthopaedics and Traumatology, Universitair Ziekenhuis Brussel (UZ Brussel), Brussels, Belgium

[3] Hand and Foot Surgery Unit (HFSU), Tournai, Belgium

Introduction

Wrist injuries are one of the most common injuries of the musculoskeletal system and may significantly impair the overall function of the upper extremity. Among the wrist injuries, lesions to the scapholunate joint are the most frequent cause of carpal instability [1, 2]. As opposed to what has previously been thought, scapholunate joint stability does not depend only on the scapholunate interosseous ligament (SLIL) but rather on both primary and secondary stabilisers forming the scapholunate ligament complex [3].

Anatomy and function of the scapholunate complex

The scapholunate complex comprises intrinsic and extrinsic elements. The intrinsic components include the three portions

of the SLIL: volar, midsubstance, and dorsal. The dorsal component is now considered the most important biomechanically. The midcarpal intrinsic ligaments consist of the palmar triquetroscaphoid (TS), the scaphotrapezial (ST) and the scaphocapitate (SC) ligaments. The extrinsic components of the scapholunate complex include the dorsal intercarpal ligament (DIC), the dorsal radiocarpal ligament (DRC) and the volar radiocarpal ligaments. Those extrinsic ligaments are considered as secondary extrinsic stabilizers. Recent anatomical studies have emphasized the key role of the DIC in scaphoid rotatory stability and of the radiocarpal ligaments in lunate stability [4–6]. Since the work of Viegas et al. in 1999 [7], demonstrating the importance of the distal and dorsal part of the SLIL and its interactions with the DIC and the DRC, anatomical studies have shown a consistent connection between the DIC and the dorsal capsular reflection, called the dorsal capsulo-scapholunate septum (DCSS) by the European Wrist Arthroscopy Society (EWAS) team. The exact role of the DCSS has yet to be determined, but early clinical experience suggests that it interacts with the other extrinsic ligaments as a secondary stabilizer of the scapholunate joint [8].

The studies of Mayfield in 1984 demonstrates that SLIL tears develop in a predictable pattern after a trauma in extension, ulnar deviation, or intercarpal supination. The palmar part of the scapholunate ligament is involved first, then the whole SLIL, then the extrinsic ligaments such as the palmar radioscaphocapitate (RSC) ligament and the dorsal radiotriquetral (DRT), sometimes called the dorsal radiocarpal (DRC) ligament, with a variable degree of ligament damage. They occur mainly in young patients of working age, who may develop wrist instability, which can eventually lead to degenerative arthritis and a scapholunate advanced collapse (SLAC) wrist. Once arthritis has developed, the treatment of these lesions is not simple and generally requires salvage procedures with a significant loss of wrist function. Early identification and treatment of scapholunate tears is advisable and also useful in understanding their anatomopathological development [9–11].

Concerning the primary and secondary stabilizers of the scapholunate (SL) joint, Short et al. showed in biomechanical studies that the intrinsic SLIL is the primary stabilizer of the SL joint, while the palmar extrinsic RSC ligament and the ST ligaments, as well as the dorsal extrinsic ligaments, DRC and DIC, contribute to the secondary stabilization of the SL joint [4, 5].

Carpal instability

According to the International Federation of Societies for Surgery of the Hand (IFSSH), carpal instability is the inability of bearing physiologic loads, without sudden changes in stress, or with a kinematic dysfunction including sudden loss of the normal carpal alignment [12].

There are four major patterns of carpal instability according to the Mayo classification: *dissociative carpal instability* (CID) or injury of one of the major intrinsic ligaments (scapholunate, lunotriquetral or capitate-hamate axial disruption); *non dissociative instability* (CIND) or injury of one of the extrinsic ligaments; *complex carpal instability* (CIC) or a combination of CID and CIND; and *adaptive carpal instability* (ACI) when the original instability is located proximal or distal from the wrist [13]. Wrist instabilities may also be classified as predynamic, dynamic or static. In *predynamic instability*, plain radiographs, clenched fist films, and fluoroscopy are negative but the instability can be diagnosed clinically by arthroscopy or CTA and MRA images. *Dynamic instability* is visible on stress views (clenched fist) and at dynamic fluoroscopic assessment but not evident on standard radiographs, while *static instability* is present when a major primary stabilizer of the joint is fully ruptured and is evident on plain radiographs [13–15].

Visualising the scapholunate complex

The role of arthroscopy

The gold standard for visualizing the SL ligaments is still arthroscopy. Wrist arthroscopy has the advantage to provide the technical capability to examine and to provide treatment at the same time. This technique allows direct visualization of the cartilage surfaces, synovial tissue and particularly the interosseous ligaments under bright light and magnification. Several authors still recommend proceeding with direct arthroscopic evaluation rather than further imaging. The portals for wrist arthroscopy are traditionally dorsal. This is in part due to the relative lack of neurovascular structures on the dorsum of the wrist as well as the initial emphasis on mainly assessing the volar wrist ligaments (Fig. 1). The portals can be divided into dorsal radiocarpal, midcarpal, distal radio-ulnar and finally volar portals. The volar portals are becoming increasingly popular, as their clinical utility has recently shown [16, 17]. Volar portals allow the visualization of the dorsal capsular structures as well as the volar aspect of the intrinsic carpal ligaments.

Geissler devised an arthroscopic classification of carpal instability with four grades, which is commonly used for SLIL injuries. In *grade I* injuries, the ligament bulges with a convex appearance as seen with the arthroscope in the radiocarpal space and loses its normal concave appearance. In the midcarpal space, the scapholunate interval is still tight and congruent. These are considered to be minor wrist sprains and usually resolve with simple immobilization. In *grade II injuries*, the SLIL continues to stretch and a convex appearance is seen between the scaphoid and the lunate with the arthroscope in the radiocarpal space. In the midcarpal space,

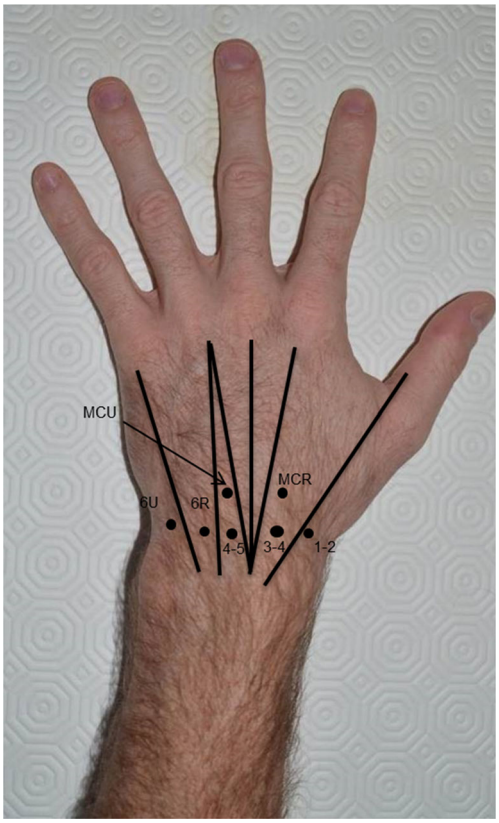

Fig. 1 Dorsal wrist arthroscopy portals. The picture displays the position of the dorsal wrist arthroscopy portals. The *black vertical lines* show the extensor tendon compartments and the *black dots* correspond to the dorsal radiocarpal (*1-2*, *3-4*, *4-5, 6R*, *6U*) portals and the dorsal midcarpal portals (*MCR*, *MCU*)

the scapholunate interval is no longer congruent. The scaphoid starts to flex palmarly and its dorsal lip is rotated distal to the level of the lunate. This is best appreciated with the arthroscope in the MCU portal. In *grade III injuries*, the SLIL tear has progressed from a stretch to a tear and a gap between the scaphoid and the lunate can be appreciated from both the radiocarpal and the midcarpal space. In the midcarpal space, the presence of the gap can be confirmed by passing a 1-mm probe between the scaphoid and the lunate. The tear usually progresses from a palmar to dorsal direction. A part of the dorsal portion of the SLIL is still attached. In *grade IV injuries*, there is a complete tear of the SLIL. The arthroscope can be freely translated between the radiocarpal and midcarpal spaces, this is called the "drive through" sign [18, 19]. The Geissler and other existing classifications, however, describe the dynamic instability of the scapholunate joint but do not distinguish the site of ligament attenuation or tear, particularly in its volar portion. More recently, the European Wrist Arthroscopy Society (EWAS) validated another more comprehensive arthroscopic classification that includes the site of the SLIL attenuation or tear [10, 20]. In grade I EWAS classification, there is no passage of the probe possible. In grade II, a lesion of the proximal/membranous part of the SLIL is present with possible passage of the tip of the probe in the SL space without widening (stable). In grade III A, a partial tear involves the palmar and proximal part of the SLIL (with or without lesion of the radiocarpal RSC- LRL ligaments) with a palmar widening on dynamic testing (anterior laxity). In grade III B, a partial lesion involves the dorsal and proximal part of SLIL (with partial lesion of the DIC ligament) with a dorsal SL widening on dynamic testing (posterior laxity). In grade III C, the SLIL tear is complete, including involvement of anterior, proximal and posterior bands (with complete lesion of one extrinsic ligament, the DIC or RSC/ LRL ligaments). Complete widening of the SL space is found by dynamic testing, reducible with removal of the probe. In grade IV, there is a complete SLIL tear including involvement of anterior, proximal and posterior bands (with complete lesion of the extrinsic ligament, the DIC and RSC/ LRL ligaments). A SL gap allows passage of the arthroscope from midcarpal to radiocarpal joints. In grade V, a wide SL gap is present with passage of the arthroscope through the SL joint and radiological abnormalities such as an increased SL gap and a DISI deformity, are seen. An additional involvement of one or more other ligaments as the triquetrohamate ligament, scaphotrapezial ligament and dorsal radiocarpal ligament can be present [10, 20].

Imaging of the scapholunate complex: current concept

Imaging modalities of the wrist joint include conventional radiography, cineradiography, arthrography, ultrasonography, computed tomographic arthrography (CTA), magnetic resonance imaging (MRI) and magnetic resonance arthrography (MRA) [21]. The diagnostic performances of these techniques, especially CTA MRI and MRA are usually appreciated in comparison to arthroscopy, which is generally considered to be the gold standard; however, because of its invasive nature, arthroscopy is not devoid of complications which have been found to occur in up to 2 %, including infection, of the injuries of the overlying tendons, nerves and arteries as well as complications due to anesthesia [21, 22].

Plain radiographs

Plain radiographs are less invasive imaging techniques; they should be obtained in different incidences (posteroanterior, lateral, navicular, and anteroposterior grip) in high quality and, when possible, completed with contralateral views for comparison. Lateral radiographs should be carefully evaluated for adequate technique. Improper positioning with supination or pronation of the wrist could indeed result in incorrect measurements of the palmar tilt. Scaphocapitate alignment is a reliable criterion to establish a reproducible neutral lateral view of the wrist. Intercarpal angles are measured to objectify perilunate subluxation or dislocation; however, measurement

of intercarpal angles on static films is difficult and subject to a great degree of variability between examiners [23]. Static SL instability is visible on standard radiographs. The indirect signs of SLIL and LT tears and possible associated extrinsic ligamentous damage include increased space between carpal bones [24], a disruption of the three arches of Gilula [24, 25] on the posteroanterior view, and carpal angle abnormalities (DISI/VISI) on the lateral view [24, 26]. The SL joint space should not exceed 2 mm on AP view. A DISI deformity is present when the lunate is abnormally rotated in extension and may be seen with a SLIL lesion. These static anomalies signify the presence of a significant and/or chronic ligamentous lesion [24, 27]. When carpal instability is suspected clinically but static radiographs are normal, *stress radiographs* should be obtained. These stress views include radial and ulnar deviation AP views, flexion and extension lateral views and a clenched-fist frontal projection [24, 27].

CT arthrography

CT arthrography (CTA) of the wrist is a technique that combines the detailed CT analysis of bony anatomy with an indirect analysis of the ligamentous wrist structures. The use of a multidetector-row CT aids to improve the reconstructions by obtaining thinner slices; therefore, CT arthrography with the use of reformatted images can provide an accurate assessment of interosseous ligament injuries and TFCC injuries [28]. As for conventional arthrography, the most sensitive technique of CTA is three-compartment injection under fluoroscopic monitoring. The contrast injection takes place in the midcarpal compartment, the radiocarpal compartment and the distal radioulnar compartment [2, 24, 29]. The choice and order of compartments for enhancement has been much debated with conventional arthrographic studies. It is acknowledged that midcarpal opacification is the most appropriate for detecting SLIL and LT tears, whereas radiocarpal opacification is useful for cartilage assessment. TFCC evaluation requires opacification of both the radiocarpal compartment and DRUJ. Although three-compartment injection technique is considered optimal, it is often possible to limit the examination to one- or two-compartment injection when spontaneous intercompartmental communication occurs and to skip the DRUJ injection in absence of ulnar-sided symptoms. Since on MDCT images, direct visualization of ligament tears is observed, identification of contrast leakage among the different compartments (radiocarpal and midcarpal for SLIL or LT tears, radiocarpal and DRUJ for TFCC tears) is less important; however, opacification on both sides of evaluated ligaments is fundamental to detect partial-thickness (noncommunicating) tears. To obtain a CTA, an iodine concentration <300 mg/ml is recommended to avoid beam-hardening artifacts. The injected volume should be sufficient to obtain a good delineation of articular structures and is typically 1–2 ml for the midcarpal compartment, 0.5–1 ml for the DRUJ, and 1–2 ml for the radiocarpal compartment [24, 30]. According to the studies of the literature, CTA has different sensitivity and specificity rates. Bille B. et al. reported that CTA of the wrist was highly accurate at detecting SLIL, LT and central TFCC tears with high sensitivity and specificity when compared to arthroscopy. For SLIL tears, the sensitivity is 85–97 % and the specificity is 79–97 % [31]. Lee R. et al. found in a cadaver study of five male wrists (with an average age of 49.6 years) a CTA sensitivity/specificity of 100 %/100 % for SLIL tears when compared to arthroscopy and arthrography [32]. More recently, Koskinen et al. investigated the potential of a dedicated extremity Cone Beam CT (CBCT) to investigate wrist ligaments. CBCT has recently been implemented in orthopedic imaging to study finger and wrist fractures as well as scaphoid fractures after screw fixation. This application offers an attractive alternative with high spatial resolution, easy installation of the patient and especially low radiation dose compared to conventional CT scanners. In their study, Koskinen et al. investigated 52 wrists to evaluate the feasibility and intra- and interobserver agreement of CBCT arthrography. Since no surgery was performed in this study, 1.5 T MRA was used as a reference. The overall mean accuracy (for SLIL, LT, TFCC tears and cartilage lesions) was 82–92 % and specificity was 81–94 %. While the sensitivity for LT and TFCC tears was 76–83 %, for SLIL tears it was only 58 %. For cartilage abnormalities, the accuracy and negative predictive value were high (90–98) [33].

Magnetic resonance imaging

Magnetic resonance imaging (MRI) is an excellent modality to diagnose hand and wrist disorders, but until now had technical limitations of spatial resolution and signal-to-noise ratio when imaging the small and intricate intra-articular structures of the wrist [28, 34]. Imaging carpal ligaments is especially difficult because these structures are thin (1–2 mm thickness) and have an oblique or curved course; therefore, inframillimetric contiguous slices are necessary to minimize partial volume effect. With the development of 3 T MR systems and 8–16 channel coils, three-dimensional (3D) sequences have shown to be more effective in analyzing carpal ligaments. Three-dimensional MRI techniques can produce much thinner contiguous slices than standard 2D sequences and their improved spatial resolution as well as the multiplanar reconstruction possibilities allow better visualization of small complex anatomical structures such as the palmar and dorsal carpal ligaments [34, 35]. Because most of the carpal ligaments have an oblique or curved course in 3D space, they often cannot be depicted in their entirety from origin to insertion, and image interpretation is based on the summation of adjacent MR slices. By applying 3D techniques with 0.5-mm-thick slices such as 3D dual echo with steady-state precession

(DESS) or fat-saturated 3D proton density (PD)-weighted sequences, this drawback could be overcome by post-processing isotropic datasets in an anatomical way [36]. Until now in the literature, few studies of MRA on 3 T compared to arthroscopy have been published, based on a small series of patients with poor sensitivity and specificity rates [37, 38]. Spaans et al. studied a larger series of 38 wrists with a clinical suspicion of SL complex injury on 3 T MR and reported improved sensitivity rates between 70 and 81 % and a specificity of 100 % for SLIL tears. The results were comparable with the 3 T MRI studies with small series published by Hobby et al. [39]. The previous comparative studies were performed on 1.5 T systems. Mak et al. found in a series of 26 patients, a sensitivity of 63 % and a specificity of 56 % for RSC tears and 25 and 67 % for LRL tears [40]. Haims et al. compared indirect MR arthrography or contrast-enhanced MRI (delayed imaging after intravenous contrast administration) and found significantly improved sensitivity rates (75–99 %) in the evaluation of the SLIL lesions when compared to unenhanced MRI [41]. Moser et al. used a technique combining CTA and MRA after injection of iodinate contrast mixed with DOTA-gadolinium and compared standard MRI, CTA and MRA. They found better sensitivity and specificity rates with MRA and good specificity rates but lower sensitivity rates with standard MRI; however, partial tears of the SLIL and the LT were significantly better visualized with MDCT arthrography [42].

Taneja et al. evaluated the prevalence of extrinsic and intrinsic ligament injuries in acute wrist traumas on MRI without arthrography; 59 % of the MR examinations was performed on a 1.5-T scanner 25 % on a 1.0-T extremity scanner and 16 % on a 3.0-T scanner. In their study, they examined 75 patients with a mean age of 42 years, and found the following results—the prevalence of extrinsic ligament injury was 75 %; the most frequently injured extrinsic ligaments were radiolunotriquetral (45 %), radioscaphocapitate (43 %), and dorsal radiotriquetral (43 %); the prevalence of intrinsic ligament injury was 60 %; the SLIL was injured in 58 % [43].

Anatomy of the scapholunate complex on MRI

The scapholunate complex comprises intrinsic and extrinsic elements.

Intrinsic ligaments

The interosseous ligaments usually have a homogeneous low signal on spin echo images, but they may have a more variable signal on gradient-recalled echo (GRE) sequences. The presence of a heterogeneous signal should not be mistaken for a tear, and could explain the poor accuracy of MRI in the diagnosis of SLIL tears in the studies of the literature [24, 44].

The SL complex comprises the SLIL, a proximal intercarpal ligament described as a cap surrounding the proximal, palmar and dorsal articular surfaces between the scaphoid and lunate. The proximal part of the ligament consists of fibrocartilage and carries the radiocarpal cartilage but does not contribute to stabilization or limitation of movements. The dorsal part of the SLIL is short and resistant, limiting translations and serving as pivot for segmental movements; while the palmar part is longer and less resistant and has some oblique fibers and limits segmental rotation [45]. MRI allows assessment of the three SLIL components and it should be assessed in all three orthogonal planes. The palmar and dorsal components are best assessed in the axial plane and the membranous segment is best assessed on the coronal plane. Oblique axial MRI may improve assessment of the individual ligament components [46, 47]. When viewed in the coronal plane, the SLIL has a triangular configuration in 90 % and linear in 10 % of the cases [45]. The dorsal and palmar components of the SLIL consist of collagen fascicles. The palmar component is differentiated from the dorsal component by being thinner and invested with loose vascular connective tissue. The membranous component of the SLIL is fibrocartilaginous without oriented collagen or neurovascular investment. The dorsal and palmar components of the SLIL are band-like. The proximal or membranous component of the SLIL varies in shape from its palmar to its dorsal aspect on coronal images. The palmar aspect of the membranous component has a trapezoidal conformation and attaches directly to the scaphoid and lunate cortex, while the central portion of the membranous component is triangular and attaches to the hyaline cartilage of the scaphoid and lunate in most cases, and the dorsal aspect of the membranous component is band-like on coronal images and is variable in attachment, attaching to the cartilage or cortex of the scaphoid and lunate in various combinations. The palmar portion of the SLIL demonstrates striated heterogeneous increased signal intensity. Similarly, the fibrocartilaginous membranous portion has been reported to predominantly demonstrate heterogeneous signal intensity, which ranges from high to intermediate signal intensity in its palmar aspect to low signal intensity in its dorsal aspect. The dorsal portion of the SLIL has low internal signal intensity, which is probably due to its constituent elements of homogeneous transversely oriented collagen fascicles [48, 49] (Fig. 2).

The midcarpal ligaments include extrinsic and intrinsic ligaments. The intrinsic midcarpal ligaments, especially the ones connecting two nonadjacent carpal bones, are often included by hand surgeons in the discussion on extrinsic ligaments. The *palmar triquetroscaphoid ligament of Sennwald* (pTS) is a palmar structure that connects the palmar surface of the triquetrum to the waist of the scaphoid, and runs below the other palmar ligaments. It appears to help maintain the carpal arch and it has not been described by many authors [45, 50]. Theumann described that the pTS arises in common with the

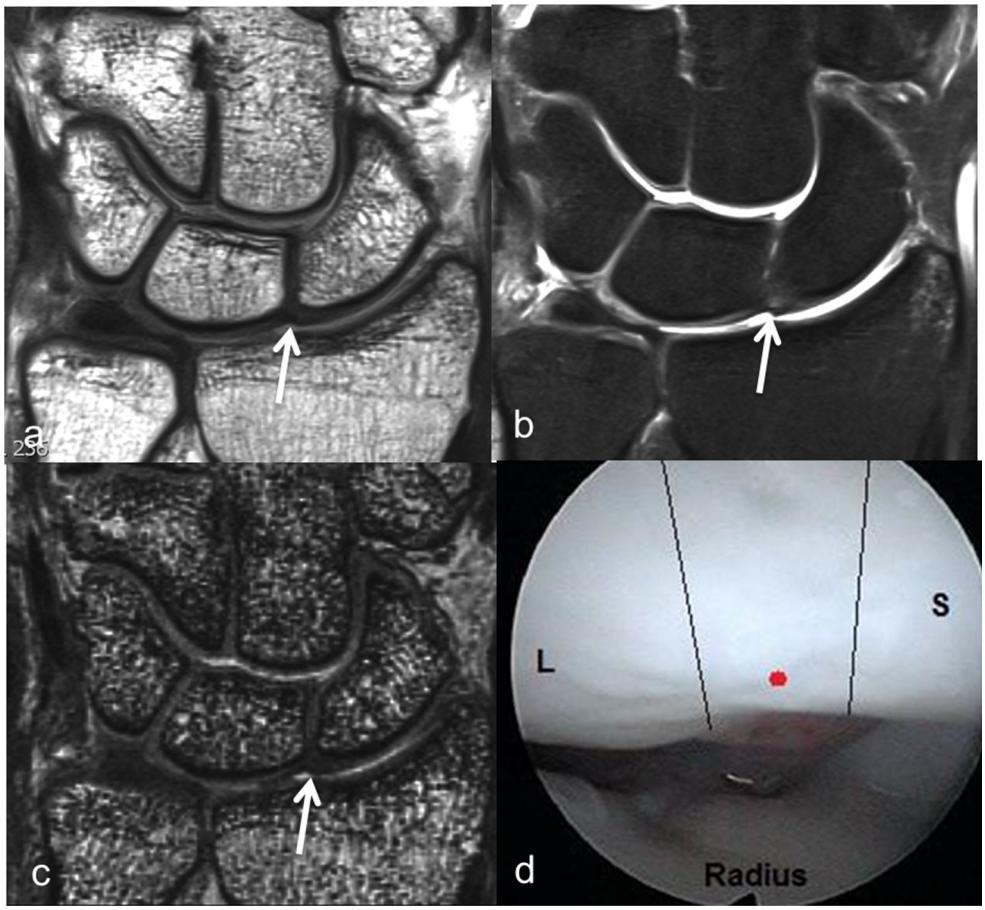

Fig. 2 **a**–**d** Normal SLIL. The SLIL is depicted on the dorsal aspect of the wrist on coronal MR images obtained with PD (**a**), fat saturated PD (**b**) and 3D DESS (**c**) sequence (*arrow*) on a patient with ulnar pain, as a thin linear hypointense structure. Arthroscopic view, from a 3-4 dorsal portal, of a normal proximal band of the SLIL (*red dot between the blacklines* in **d**). *S* Scaphoid, *L* Lunate

fibrous band of the radioscaphocapitate (RSC) ligament from the scaphoid and extends distally as two parallel bands. The proximal band runs directly to the triquetrum and the distal band forms an arch and inserts into the palmar aspect of the capitate (distal to the RSC ligament), the palmar aspect of the hamate, and the triquetrum (below the pisohamate ligament) in common with the proximal band. Both bands insert on the palmar aspect of the triquetrum distal to the RLT ligament. The distal band of the palmar scaphotriquetral ligament is also known as the v-shape ligament, with a radial (scaphocapitate) and an ulnar (capitotriquetral) arm [51]. According to Sennwald, the pTS ligament avoids palmar triquetroscaphoid dissociation and, indirectly, scapholunate dissociation. It maintains the proximal part of the capitate when the wrist extends [52]. The ligament is extra-articular and not directly accessible to arthroscopic examination. It may be visualised on 2-mm-thick MR images obtained in the axial plane using T1 or PD spin echo sequence or better on 0.5-mm-thick contiguous axial reconstructions from 3D DESS or fat-saturated 3D PD sequences. It usually presents a dark hypointense signal and a slightly oblique course on axial views [36] (Fig. 3).

A *scaphotrapezial ligament complex* is described by Drewniany et al. and consists of four components: a strong scaphotrapezial ligament (consisting of a radial and an ulnar slip), the palmar and dorsal capsules, and the dorsal scaphocapitate ligament, being directly related in resisting the diastasis of the scaphotrapezoid trapezial (STT) joint. These investigators prove that the scaphotrapezial ligament is the major anatomic stabilizer of the STT joint. It also appears to be a secondary stabilizer of the scapholunate joint [53, 54]. The palmar scaphotrapezial (ST) ligament runs from the radial side of the scaphoid to the palmar and radial side of the trapezium. Both MRI and MRA show the radial slip of the pST ligament as a short interosseous band that traverses the STT joint, linking the scaphoid tuberosity with the ridge of the trapezium. The ligament has a relatively low signal intensity on most sequences. The use of intraarticular contrast media increases the sensitivity for detecting those ligaments by improving the differentiation between the injured ligaments and surrounding structures and due to a better contrast resolution. The ligaments are better visualized on the high-resolution sequences which allow 3D reformations, especially using 3 T scanners [54] (Fig. 4c,f).

At the dorsal side, there is a midcarpal ligament, called the *dorsal intercarpal ligament* (DIC) including the *dorsal triquetroscaphoid* (dTS) and *triquetro-trapezoido-trapezial* (TTT) ligament. The DIC is the third secondary stabilizer of the wrist. It unites the triquetrum and the distal scaphoid.

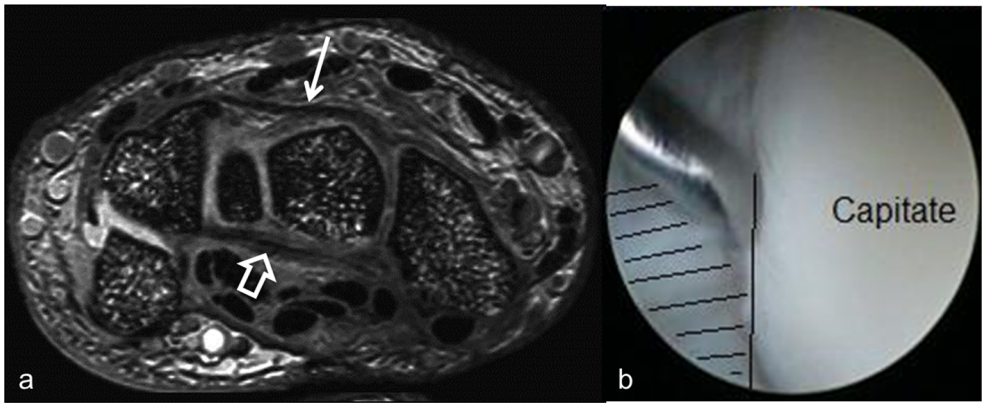

Fig. 3 **a**–**b** Normal palmar triquetroscaphoid ligament of Sennwald (pTS) and dorsal triquetroscaphoid (dTS) or dorsal intercarpal ligament (DIC). 3D DESS axial reconstruction (**a**) shows a normal pTS (*open arrow*) and a normal DIC (*arrow*), both having a dark hypointense signal and a slightly oblique course. The dTS is depicted on arthroscopy, after shaving, from a 1-3 midcarpal portal (**b**) underneath the probe in the *shaded area*

Numerous morphological variants are visualised on cadaveric specimens. The dTS and TTT often originate together and separately at the distal insertion, some of the fibers extending onto the trapezium and trapezoid. When the dTS and TTT originate separately on the triquetrum, together with the extrinsic dorsal radiotriquetral ligament, they form a V-shaped structure with its apex at the level of the ligamentous crest of the triquetrum. These ligaments are clearly seen on coronal and axial images (Figs. 3 and 5).

Since the work of Viegas et al. in 1999 [7], demonstrating the importance of the distal and dorsal part of the SLIL and its interactions with the DIC and the DRC, anatomical studies have shown a consistent connection between the DIC and the dorsal capsular reflection, called the "dorsal capsuloscapholunate septum" (DCSS) by the EWAS team. The DCSS is a fibrous structure that connects the dorsal capsule, the DIC and the SLIL. It is a thin distinct structure that is separated from the insertion of the dorsal capsule on the scaphoid and lunate. It arises from the dorsal capsule and inserts in a bifid way at the bone-ligament junction of the dorsal superior aspect of the scaphoid and lunate. In the sagittal plane, the DCSS is oriented obliquely in a distal and palmar direction [8] (Fig. 6e).

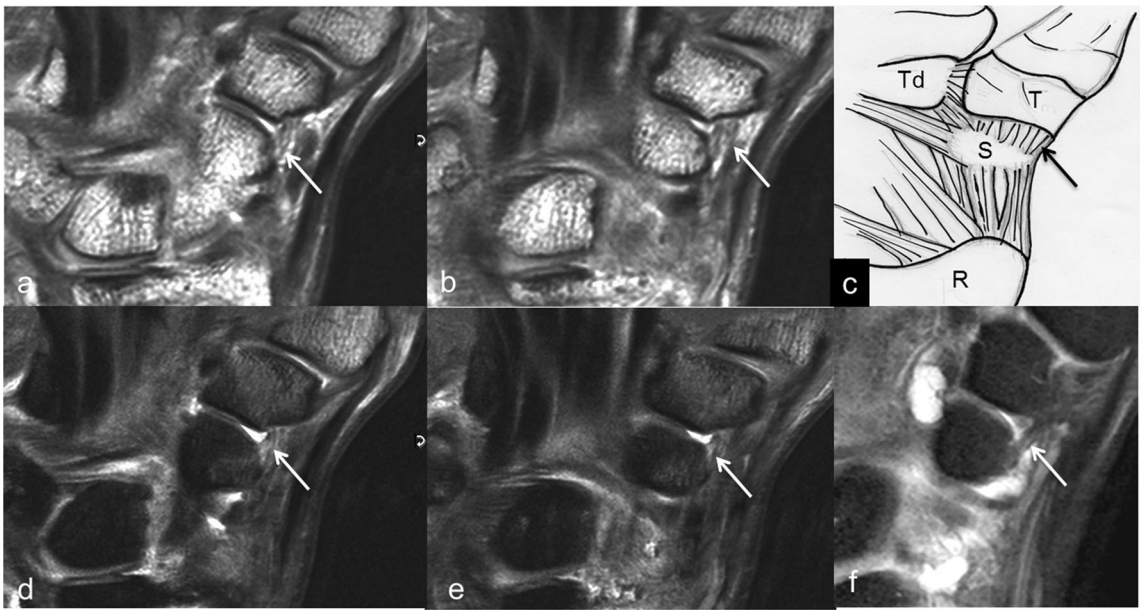

Fig. 4 **a**–**f** Normal and sprained scaphotrapezial ligament (pST) PD- (**a**–**b**) and fat saturated PD-weighted (**d**–**e**) coronal images of the palmar aspect of the wrist obtained with 3 compartment MRA show an elongation of the scaphotrapezial ligament as described at arthroscopy. The ligament has an increased signal intensity on both sequences with slight nonhomogeneous infiltration (**a**,**b**,**d**,**e**, *arrow*). Compare with a fat saturated PD-weighted coronal image of a normal radial slip of the pST ligament (**f**) and a drawing of the ST ligament (**c**, *arrow*). *S* scaphoid, *Td* trapezoideum, *T* trapezium, *R* radius

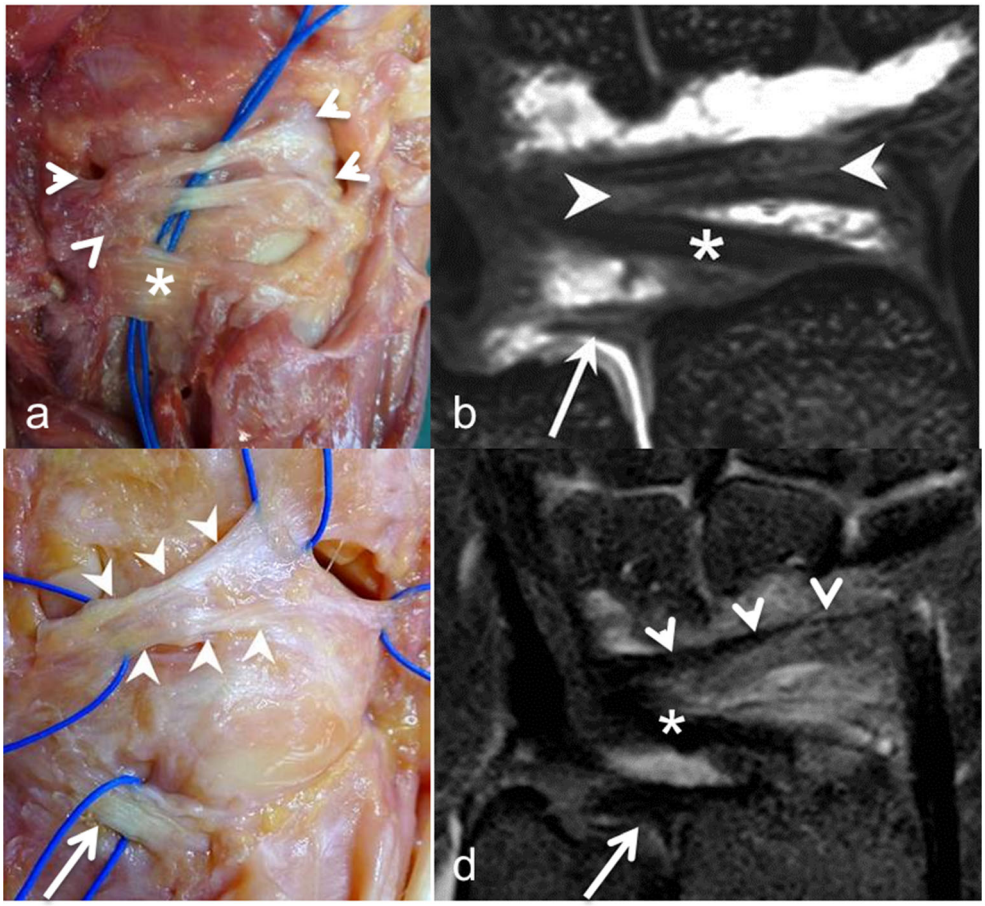

Fig. 5 **a**–**d** Normal anatomical variants of the dorsal midcarpal ligaments. Two main anatomical variants of the dorsal intercarpal ligament are demonstrated on cadaveric specimens and on 0.5-mm-thick coronal 3D DESS images. In **a** and **b**, the dorsal triquetroscaphoid and the triquetro-trapezoido-trapezial ligaments (*arrowheads*) are separated. In **c** and **d**, they merge together (*arrowheads*). The dorsal radiotriquetral (* in **a**,**b**,**d**) and the dorsal radio-ulnar ligament (*arrow* in **b**–**d**) are also shown

Extrinsic ligaments

Those are intracapsular but extrasynovial structures and connect the radius and the ulna to the carpal bones. They are enveloped within a continuous superficial fibrous portion of the joint capsule, and their deep surfaces are enveloped by synovium. They consist of radiocarpal and ulnocarpal ligaments, both at the palmar and dorsal aspect of the wrist. Palmar ligaments are thicker and stronger than dorsal ligaments. Functionally, the ligaments can be divided into three reversed V-shaped groups, two on the palmar side and one on the dorsal side [36, 55]. All radiocarpal ligaments have a proximal origin at the distal end of the radius and a distal insertion at the level of one or more carpal bones. They correspond to areas of capsular thickening. Most have an oblique orientation, and several adjacent slices are required to analyze the entirety of the ligament. They appear as fasciculate and striated structures, presenting bands of low signal intensity alternating with bands of intermediate or high signal intensity on coronal slices, which corresponds to strong fascicles separated by loose connective tissue in dissected cadaveric wrists [34, 56].

There is one dorsal extrinsic ligament, which is called the dorsal radiocarpal (DRC) or dorsal radiotriquetral ligament. As previously mentioned, the DRC and the DIC form a V with the apex oriented toward the triquetrum [56]. The DRC is a single 1-mm-thick band extending from the dorsal part of the distal radius (next to or on the Lister tubercle and/or the radial styloid process). Both bands insert on the dorsal aspect of the triquetrum distal to the RLT. It is easily identified on thin coronal and sagittal fat-saturated 3D PD or 3D DESS reformatted images, inferior to the DIC and forms the dorsal component of the "Kuhlman sling". The DRC limits intracarpal supination, radial deviation, palmar flexion, and ulnar translation of the carpal bones. It helps to stabilize the lunate dorsally and limits the extent of ulnar translation of the wrist. The ligament is most often well visualized on thin coronal 3D images [36, 57, 58].

The main extrinsic ligament located at the palmar side of the scapholunate joint is the *radioscaphocapitate* (RSC) ligament, which is a large and strong ligament that originates from the styloid process of the radius, envelops the scaphoid waist where some fibers also insert, to attach on the palmar tubercle of the capitate. It helps maintain the position of the scaphoid, while acting like a seat belt and is crucial in scaphoid stability, and a secondary stabilizer of the SL joint [59–61]. According to Berger, only 10 % of the fibers insert on the capitate. The proximal RSC is the visible radiocarpal portion of the ligament at arthroscopy, which is located radially relative to the

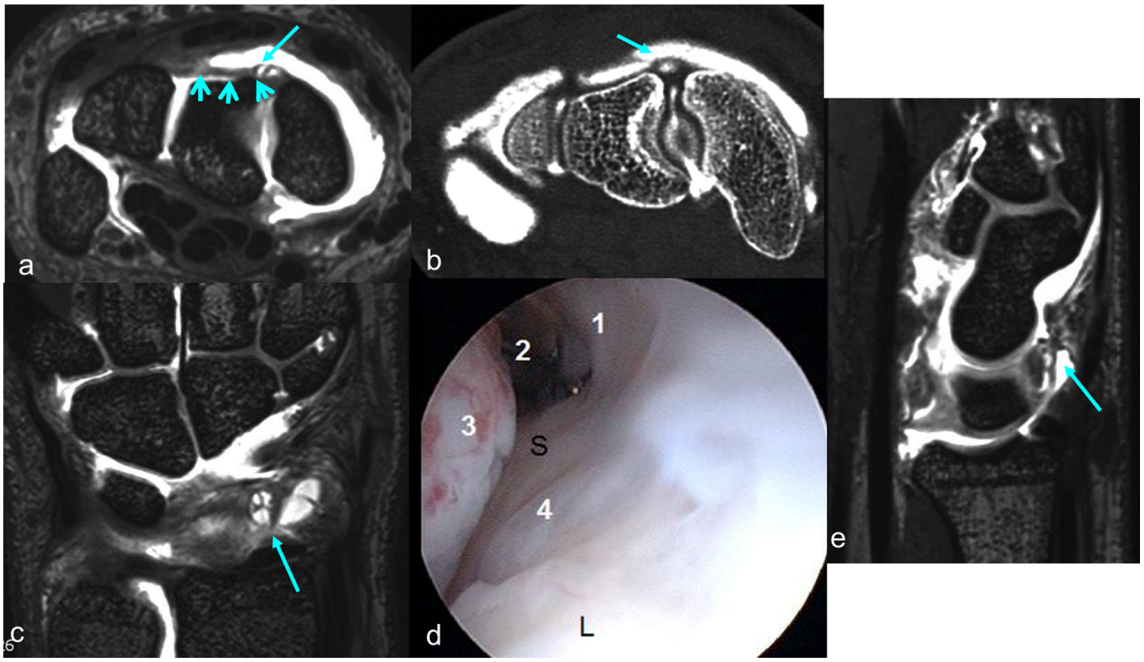

Fig. 6 **a**–**e** Sprain of the dorsal capsulo-scapholunate septum (DCSS) with small cyst. Axial MRA reconstruction using 3D DESS sequence and CTA depict the cystic appearance of the DCSS (**a**–**b**, *arrow*) within the dorsal midcarpal triquetroscaphoid ligament (dTS, arrowheads in **a**). On the coronal section, the inframillimetric cyst is located within the dorsal capsule (**c**, *arrow*). The sagittal MRA reconstruction demonstrates the DCSS connecting the SLIL and the dorsal capsule (**e**, *arrow*). The arthroscopic view, from a 6R dorsal radiocarpal portal (**d**) depicts the DCSS (*1* in **d**). *2* microkyste, *3* dorsal hemorrhagic synovitis, *4* dorsal band of the SLIL. *S* scaphoid, *L* lunate

LRL, from which it is separated by the interligamentous sulcus, readily seen between these two ligaments on coronal and sagittal slices. The distal RSC is the midcarpal portion of the ligament and is visible at arthroscopy on the ulnar part of the scaphoid. Because of the relatively large size and obliquity of the RSC, the normal configuration and course can usually be visualized on three to four contiguous 0.5-mm-thick coronal slices. The RSC can also be identified in the sagittal plane; it is seen palmar to the waist of the scaphoid, being distal to the long radiolunate ligament and arising from the palmar aspect of the radius and inserting into the distal pole of the scaphoid [4, 62].

A small extrinsic ligament is found at the palmar side of the scapholunate joint, and is referred to as the *radioscapholunate* (RSL) ligament (or ligament of Testut). It originates between the short and long radiolunate ligaments, deeper than the RSC and has fibers embedded in the SLIL. According to Berger, it is not a true ligament in the biomechanical or histological sense, and can be considered a mesocapsule. It corresponds to a rather loose and thin fibrous structure, similar to a synovial fold. Histologically, the RSL has loosely organized collagen fibers and contains neurovascular structures supplying the SLIL, which may explain its often reddish hemorrhagic appearance at arthroscopy when an associated injury of the

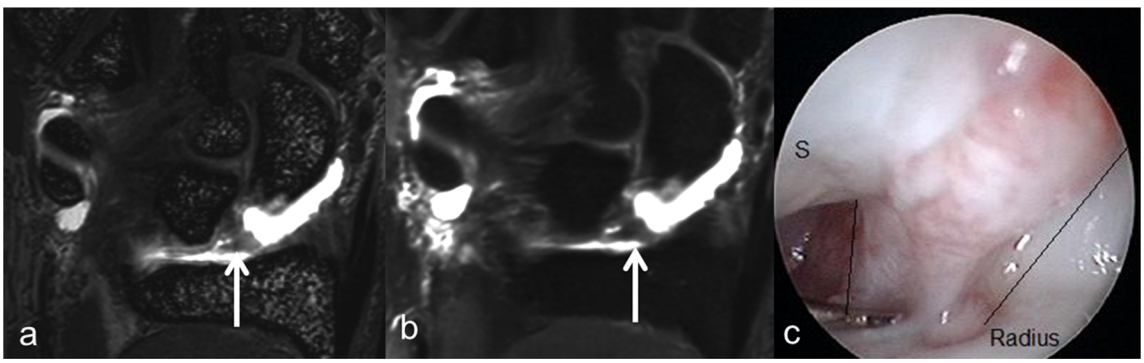

Fig. 7 **a**–**c** Normal radioscapholunate ligament or ligament of Testut (RSL). On palmar coronal 3D DESS (**a**) and fat saturated 3D PD (**b**) images, the normal RSL presents an intermediate to dark signal intensity without apparent striations and with a less organized rather loose appearance, as a synovial fold (*arrow*). On arthroscopy from a radiocarpal portal (**c**), it appears like a veil in front of the SLIL in presence of physiological synovitis. It has a *reddish* appearance probably because of the neurovascular content of the RSL (delimited by the oblique lines on **c**). *S* scaphoid

surrounding ligaments is observed. Because its fibers merge with those of the SLIL, these two structures cannot easily be differentiated on MR images. The ligament may present areas of mixed high and intermediate signal intensity, without apparent striations and with a less organized appearance, compared with the other palmar ligaments. Rominger et al. observed a dark ligament-like structure connecting the palmar aspect of the radius with the scaphoid and the lunate in 65 % of cases [58]. Since it runs superficial to the SLIL, it is used by surgeons as an arthroscopic landmark to help locate the SLIL, which may be difficult to identify. It can sometimes obscure the anterior part of the radiocarpal joint like a veil, especially when a synovitis is present [36, 63] (Fig. 7).

Pathology of the scapholunate complex on MRI

Tears of the wrist ligaments are diagnosed on the basis of MRI findings of irregular morphology, abnormal signal intensity, and fluid partially or completely transecting the ligamentous structures. Accurate assessment of wrist ligament injury with

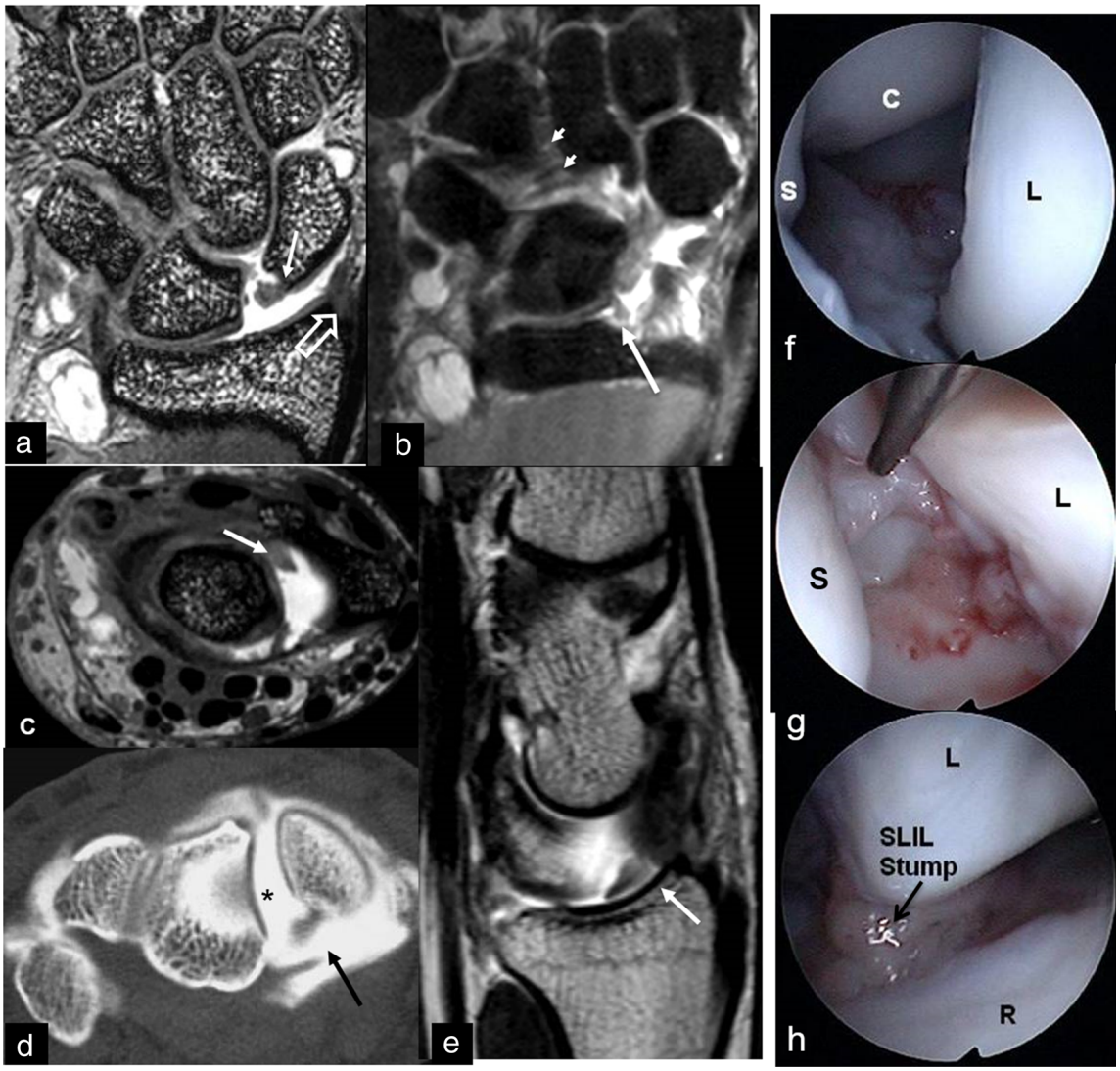

Fig. 8 **a**–**h** Disrupted scapholunate interosseous ligament (SLIL) and distal radioscaphocapitate (RSC) ligament. The consecutive palmar coronal images obtained with 3 compartment magnetic resonance arthrography (MRA) using a 3D DESS (**a**) and a fat-saturated proton density (PD) sequence (**b**) demonstrate a contrast extravasation from radiocarpal to midcarpal, indicating a complete disruption of the SLIL. There is a clear widening of the scapholunate space with the scaphoid stump hanging free (**a**, *arrow*). A thickening of the proximal attachment of the RSC is seen on the radial styloid (**a**, *open arrow*). The most palmar coronal image (**b**) depicts the RSL ligament (*thin arrow*) and the midcarpal triquetrocapitate ligament (**b**, *arrowheads*). The remnant of the dorsal band is recognized on a thin 0.5-mm axial reconstruction from a 3D DESS data set obtained in the coronal plane (**c**, arrow) and on a 2-mm sagittal T2-weighted image through the scapholunate space (**e**, *arrow*) . The palmar stump of the SLIL is surrounded by contrast on an axial 3 compartment computed tomographic arthrography (CTA) (**d**, *arrow*). The scapholunate space is widened and filled with contrast (**d**, *). Arthroscopic views from a dorsal radiocarpal portal demonstrate a large widening of the scapholunate space with easy passage of the scope from radiocarpal to midcarpal (**f**–**g**). The palmar SLIL stump is visualized on the view from the dorsal 3-4 portal (**h**, *arrow*). *S* scaphoid; *C* capitate; *L* lunate; *R* radius

MRI is often difficult. Factors that contribute to this difficulty in diagnostic assessment include low image resolution, low signal-to-noise ratio, low contrast resolution, normal variant morphology of the ligaments, and normal variant internal signal intensity. Because the diagnosis of ligament injury is based on recognition of abnormal morphology and signal intensity at MRI; a lack of familiarity with normal variant anatomic MRI appearances may contribute to the suboptimal sensitivity and specificity for lesion detection. Therefore, it is important to become familiar with the morphology and signal intensity at high-resolution MRI to improve the accuracy of diagnosis of ligamentous disease. [49] As previously described, the SLIL has a horseshoe shape subdivided into palmar, proximal (membranous) and dorsal components. The palmar band is the most vulnerable, especially at the site of scaphoid attachment. The proximal membranous part is subject to degenerative central perforation especially in the elderly, which is usually asymptomatic. The dorsal band of the SLIL is the thickest, strongest, and most functionally important. Complete SLIL disruption or involvement of either the dorsal or the palmar band is suggestive of trauma. Tears of the dorsal band are often symptomatic and can lead to wrist instability.

The proximal membranous part of the SLIL is best depicted on mid-coronal images, while the dorsal and palmar bands can be evaluated on respectively dorsal and palmar coronal sections but better demonstrated on axial MRA or

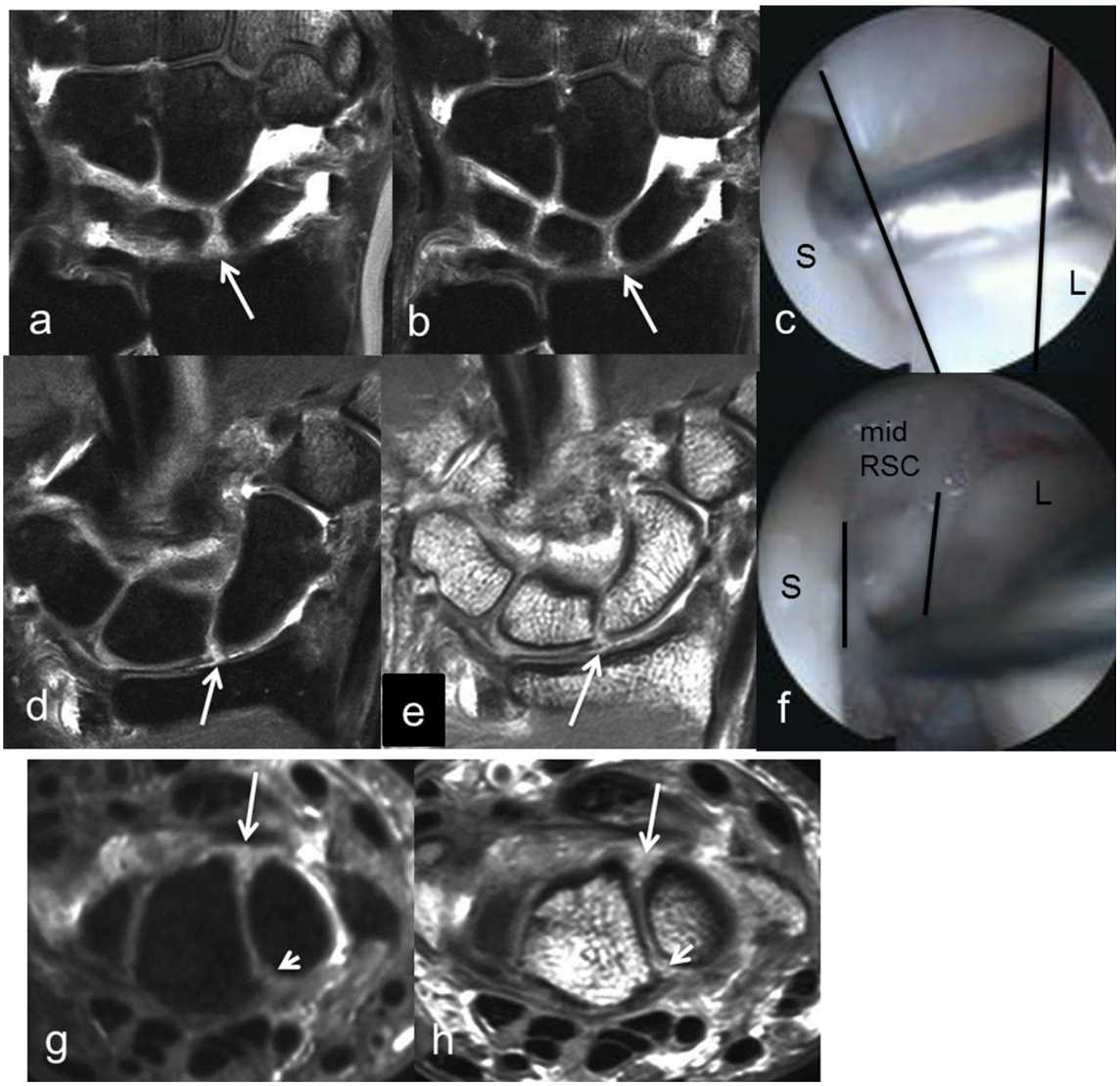

Fig. 9 **a**–**h** Complete scapholunate interosseous ligament (SLIL) rupture. Dorsal consecutive 2-mm-thick fat-saturated PD-weighted images depict an increased signal intensity of the dorsal band of the SLIL (**a**) and a tear at the scaphoid attachment (**b**). In arthroscopy (**c**), the free edge of the detached dorsal band (delimited by the *two vertical lines*) is hooked by the probe. Palmar fat saturated PD (**d**) and PD without fat saturation (**e**) as well as the arthroscopic view from a midcarpal portal (**f**, delimited by the *small black lines*) demonstrates a detachment of the palmar band from the scaphoid insertion. *S* scaphoid; *L* lunate; *mid RSC* midcarpal part of RSC. Chronic complete tear of dorsal (*arrow*) and palmar (*short arrow*) SLIL on axial fat saturated PD- (**g**) and PD-weighted (**h**) images with discontinuity and increased signal intensity. No widening of SL space is seen on either MR images

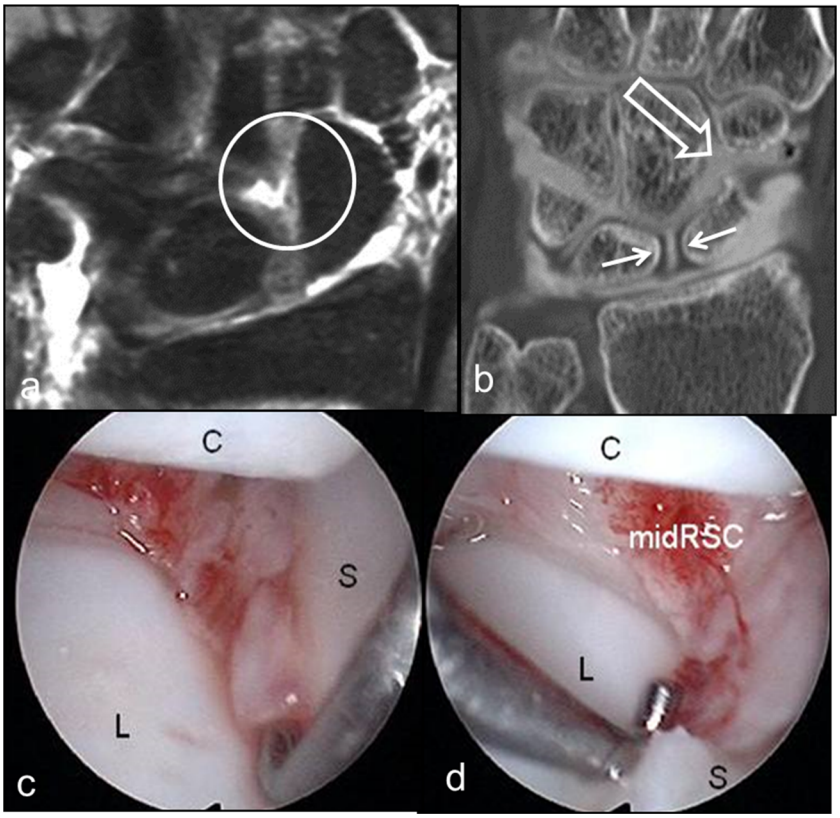

Fig. 10 **a**–**d** Tear of the distal part of the radioscaphocapitate ligament (RSC) associated to a rupture of the palmar band of the scapholunate interosseous ligament (SLIL). A coronal reconstruction from a 3D fat-saturated PD sequence demonstrates high signal contrast fluid in the midcarpal space (between the capitate and the SLIL) (**a**, *circle*). A coronal reconstructed CTA image discloses contrast extravasation through the scapholunate joint, from midcarpal to radiocarpal joint (**b**, *arrows*).The contrast extends through the scaphocapitate joint suggesting a distal RSC lesion (**b**, *open arrow*). Arthroscopic views of the corresponding patient, from a dorsal midcarpal ulnar portal (MCU), confirm an anteriorly widened scapholunate space due to the SLIL palmar band rupture (**c**). The partially ruptured and hemorrhagic distal RSC is visualized in **d**. *S* scaphoid; *C* capitate; *L* lunate

CTA images. Pathologic changes are best seen on images obtained with fluid-sensitive fat-suppressed sequences. The bands of the SLIL are better visualized when using a 3 T MRI scanner and a 8–16 channel wrist coil which allows their positioning at the isocenter of the coil [45]. Avulsive cystic changes at the osseous attachment sites of the SLIL components, soft tissue ganglion formation, and scapholunate dissociation (scapholunate distance >2 mm) seen on 3 T MR images are suggestive of a tear. Dorsal or volar intercalated segmental instability are secondary to SLIL tears, those are difficult to detect on MR images because the wrist is not stressed. The imaging planes can be transposed at the PACS (picture archiving and communication system) workstation to obtain the scapholunate angle. Complete tears of the

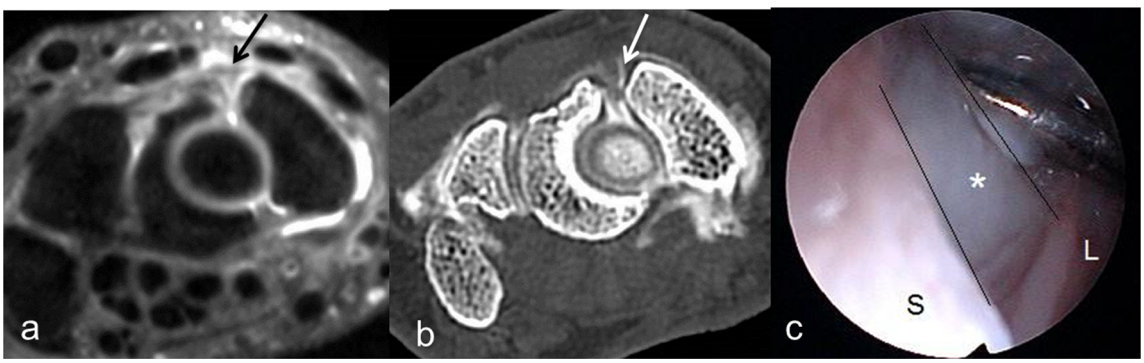

Fig. 11 **a**–**c** Lesion of the dorsal capsulo-scapholunate septum (DCSS). A detached DCSS is shown on a thin 0.5-mm axial reconstruction from a 3D fat saturated data set obtained in the coronal plane (**a**, *arrow*) and on 3 compartment CTA (**b**, *arrow*). The same lesion is demonstrated on arthroscopy with the probe in the torn DCSS (**c**, *asterisk between the 2 oblique black lines*). *S* scaphoid, *L* lunate

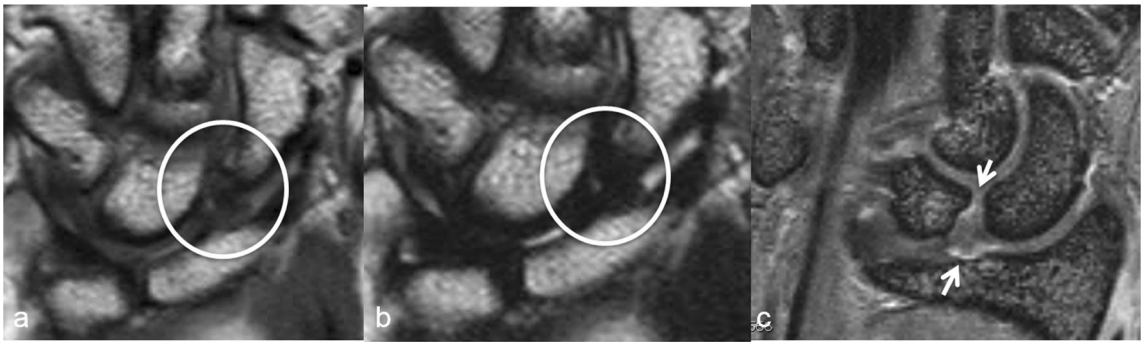

Fig. 12 **a**–**c** Chronic sprain of the SLIL on a plain MRI compared to an indirect MRA with intravenous (iv) contrast. On the plain MRI without contrast with PD- (**a**) and T2-weighted (**b**) coronal images, the SLIL (*encircled*) appears amorphous and thickened by fibrous scar tissue (with inhomogeneous signal on PD and low signal on T2). On the coronal MR image obtained after iv injection (**c**), contrast enhancement corresponding to granulation tissue is disclosed around the sprained palmar band of the SLIL (*arrows*)

interosseous ligaments appear as distinct areas of ligament discontinuity, morphological distortion, contrast extravasation or rarely as nonvisualization of the ligament [36, 64]. A ligament stump can be shown hanging free at the scaphoid or lunate site of detachment. MR images with intravenous or intra-articular contrast using 2-mm fat-saturated PD sequence or thin 3D DESS (Fig. 8a) or fat-saturated 3D PD (Fig. 8b) can demonstrate a contrast extravasation from radiocarpal to midcarpal indicating a complete disruption of the SLIL. This can be associated or not to widening of the scapholunate space. Arthroscopy may show a large widening of the scapholunate space with easy passage of the scope from radiocarpal to midcarpal (Figs. 8 and 9). Partial tears of the interosseous ligaments appear as focal thinning, changes in signal intensity, contour irregularity and waviness. On MRA and even better on CTA images (thanks to the higher differentiation between the injected contrast and the grey soft tissue background), contrast extravasation through the scapholunate joint at the level of one of the SLIL bands indicates a full-thickness tear of the palmar or dorsal band (Fig. 10). Full-thickness tears of one segment (usually communicating) might be differentiated from partial-thickness (noncommunicating) tears on CTA [30] (Fig. 11). In more chronic lesions, the SLIL can be amorphous and infiltrated by fibrosis and scar tissue (with low signal intensity on T2-weighted sequences) after healing. The fibrous scarring can obstruct the scapholunate space and lead to a negative arthrogram. On indirect MRA (with intravenous injection prior to the MR examination), a periligamentous contrast uptake can be shown corresponding to granulation tissue associated with fibrous scar tissue infiltration of the injured ligament. Ligament scarring after a sprained SLIL has less valuable mechanical properties explaining persisting pain even if the wrist is not clinically unstable. Diagnosis of fibrotic changes of sprained ligaments might change treatment decisions [45] (Figs. 12 and 13).

Injury of the *radioscaphocapitate ligament* is usually associated with a rupture of the intrinsic SLIL, which may lead to scaphoid instability with DISI deformity and a scapholunate gap on radiographs. As other injured radiocarpal ligaments, RSC ruptures may include nonvisualization, abnormal signal and abnormal thickness. A segmental defect can be detected as in distal RSC detachment with visualization of a remnant of the RSC at the midcarpal insertion on thin 3D DESS images

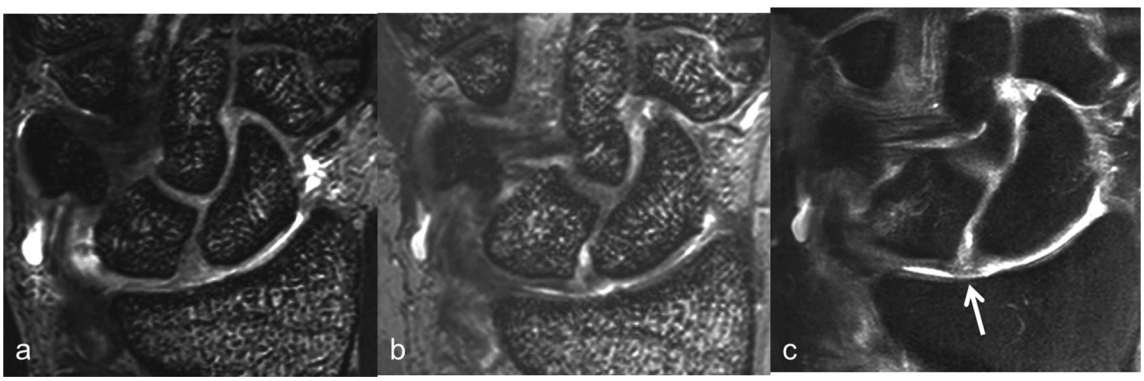

Fig. 13 **a**–**c** Chronic painful partial-thickness SLIL tear on direct compared to indirect MRA. MR arthrographic coronal 0.5-mm-thick image obtained with 3D DESS sequence (**a**) shows a thickened SL without contrast leakage and perforation (corresponding to a negative MRA). On the contrary, the 0.5-mm-thick 3D DESS (**b**) and 2-mm-thick fat-saturated PD (**c**) obtained after iv injection demonstrate a contrast enhancement, corresponding to an inflammatory synovitis, with a small partial tear within the painful chronically injured SLIL

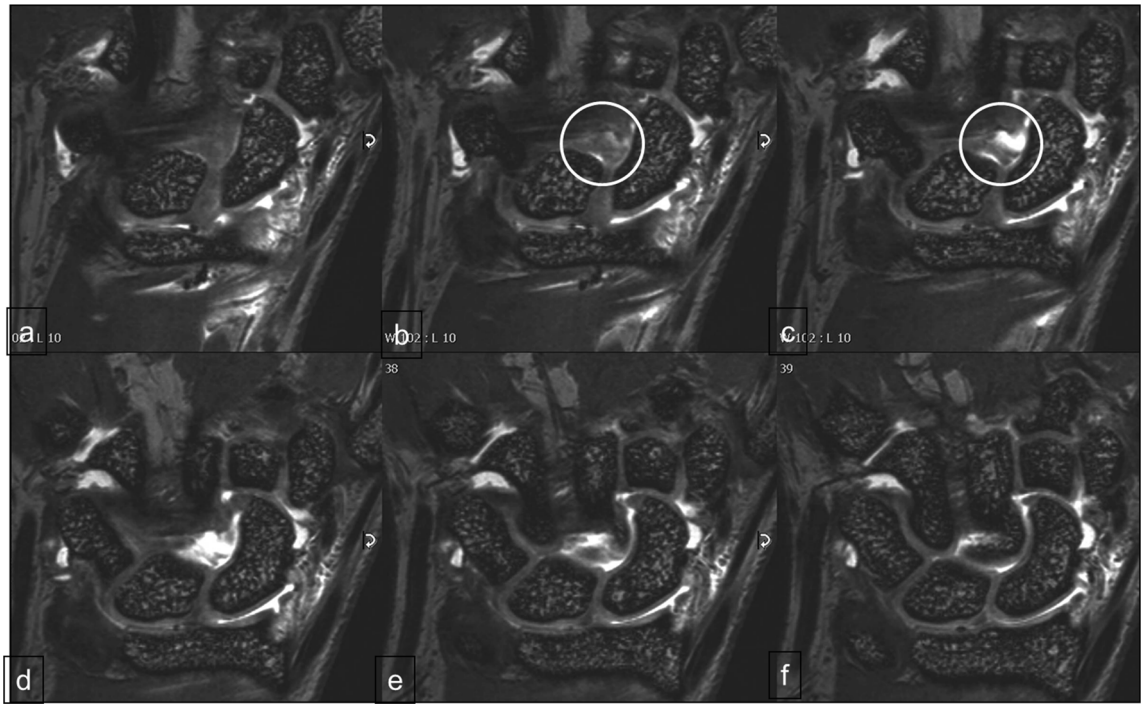

Fig. 14 **a**–**f** Detachment of the midcarpal or distal part of the radioscaphocapitate ligament (RSC). The consecutive palmar coronal images obtained with 3 compartment MRA using a 3D DESS sequence show the remnant of the distal RSC close to the capitate attachment (*circled* in **b**–**c**)

(Fig. 14). In partial ruptures, the RSC ligament can show an interruption of part of the fibers with irregular frayed outlines or a wavy appearance and an abnormal heterogeneous signal.

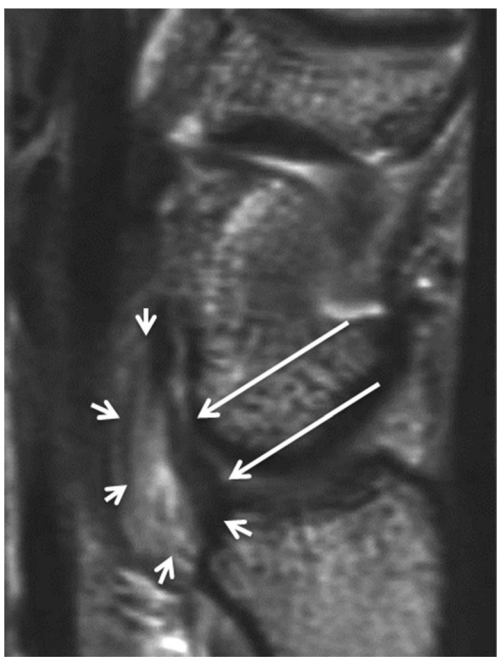

Fig. 15 Sprained proximal attachment of radioscaphocapitate ligament (RSC). A 2-mm-thick sagittal fat saturated PD image shows a RSC ligament (*long arrows*) with irregular outline and abnormal proximal infiltration associated with periligamentous synovitis in front of the radioscaphoid joint line (*arrowheads*)

The interligamentous sulcus could be filled by hyperemic synovitis on MR images as in arthroscopy. The injured ligaments may also be obscured and covered by synovitis on sagittal 2-mm thick fat-saturated PD images (Figs. 15, 16 and 17). In the chronic phase, fibrous thickening of the ligament with surrounding scar tissue may be demonstrated with heterogeneous signal on PD and low signal intensity on T2-weighted images [36].

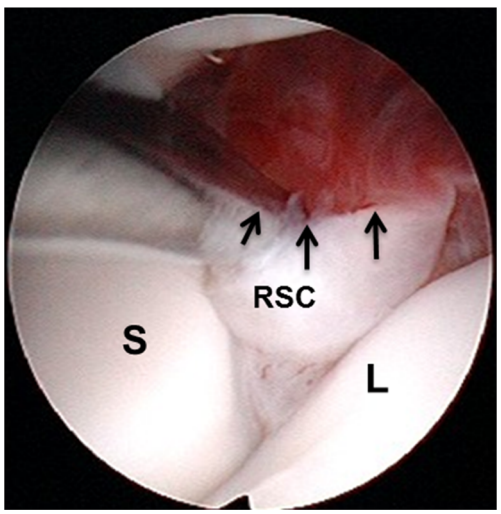

Fig. 16 Complete rupture of the midcarpal attachment of the radioscaphocapitate ligament (*RSC*). Arthroscopic view from a dorsal ulnar midcarpal portal showing the hemorrhagic synovitis and avulsion, palpated with the hook, of the midcarpal RSC (*arrows*) insertion. *S* scaphoid; *L* lunate; *RSC* radioscaphocapitate ligament

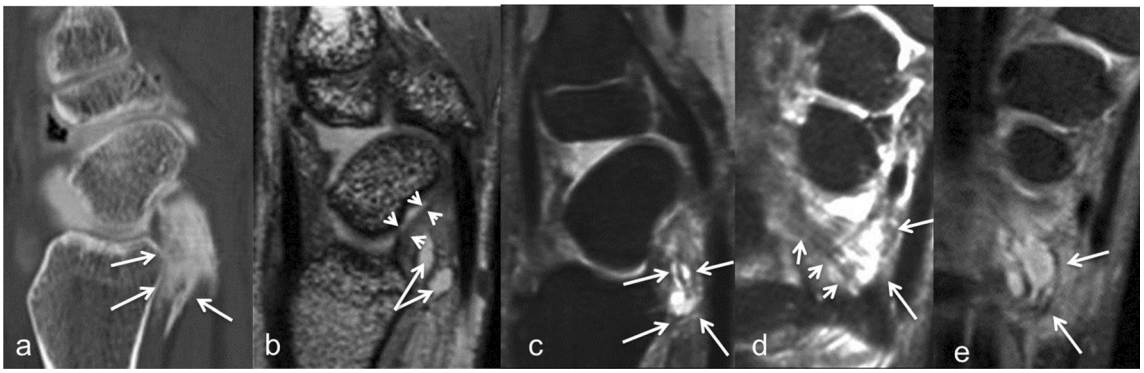

Fig. 17 **a**–**e** Sprained proximal radioscaphocapitate ligament (*RSC*). Contrast extravasation is noticed in front of the distal radial epiphysis on a sagittal reconstructed CTA image (**a**, *arrows*) suggesting the presence of a proximal RSC lesion. On thin 0.5-mm-sagittal reconstructions from a 3D DESS (**b**) sequence and a 3D fat saturated PD (**c**) sequence, a periligamentous infiltration (**b**, *arrowheads*), fraying and cystic synovial distension in volar and inferior to the proximal RSC (**b**–**d**, *arrows*). Coronal 3D fat saturated PD sequence (**d**–**e**) shows the normal striation of the RSC (**d**, *short arrows*) and the cystic distension inferior to the RSC (**d**–**e**, *arrows*)

The DRC and DIC ligaments are frequently injured during a fall on an outstretched hand, producing a dorsal wrist sprain. Before the advent of MRI, the dorsal carpal ligaments were difficult to visualize without surgical exploration. Ligamentous injuries were diagnosed on the basis of clinical signs and symptoms or indirectly by detecting abnormal carpal motion. Previous reports on MRI of the dorsal ligaments described inconsistent segmental visualization with 2D and 3D imaging techniques. An abnormal dorsal ligament may present similar to other injured ligaments with a frayed outline and may appear slightly loose or retracted with surrounding hypointense fibrous scar infiltration on T2. This may occasionally lead to dorsal impingement, which is a clinical conflict with chronic pain and swollen dorsal capsular wrist structures in repetitive dorsal hyperflexion. Associated dorsal ganglion cysts may be seen within or along the dorsal capsular ligaments and exhibit high signal on fat-saturated T2-weighted and 3D DESS axial, coronal and sagittal images [36, 56, 58]. In our experience, a traumatic detachment of the DCSS (as described in the preceding as the connection between the DIC ligament and the dorsal capsular reflection covering the distal and dorsal segment of the SLIL) can be associated with the presence of a cystic distension within the DCSS [8] (Figs. 6 and 11).

Conclusion

Direct imaging of anatomy and pathology of the ligaments of the scapholunate complex needs MRA using 3D sequences with 0.5-mm-thick slices and multiplanar reconstructions on 3 T scanners. CT arthrography affords indirect imaging of part of those ligaments. Signs of post-traumatic ligament pathologies described in MRA examinations include contrast extravasation, discontinuity, nonvisualization, changes in signal intensity, contour irregularity with waviness and periligamentous infiltration.

Based on this preliminary experience, we believe that advanced 3 T MRA is capable of evaluating the scapholunate complex and could help to reduce the number of diagnostic arthroscopies in the future. Prospective correlation studies with comparison to arthroscopic findings need to be performed to determine the reliability of 3D fat-saturated PD and 3D DESS MR sequences in the diagnosis of injuries of the scapholunate complex.

Conflict of interest The authors declare that they have no conflict of interest.

References

1. Manuel J, Moran SL. The diagnosis and treatment of scapholunate instability. Orthop Clin N Am. 2007;38(2):261–77.
2. Kuo CE, Wolfe SW. Scapholunate instability: current concepts in diagnosis and management. J Hand Surg [Am]. 2008;33(6):998–1013.
3. Slutsky D. Current innovations in wrist arthroscopy. J Hand Surg [Am]. 2012;37(9):1932–41.
4. Short WH, Werner FW, Green JK, Masaoka S. Biomechanical evaluation of ligamentous stabilizers of the scaphoid and lunate. J Hand Surg [Am]. 2002;27(6):991–1002.
5. Short WH, Werner FW, Green JK, Sutton LG, Brutus JP. Biomechanical evaluation of the ligamentous stabilizers of the scaphoid and lunate: part III. J Hand Surg [Am]. 2007;32(3):297–309.
6. Cambon Binder A, Kerfant M, Wahegaonkar AL, Tandara A, Mathoulin A. Dorsal wrist capsular tears in association with scapholunate instability: results of an arthroscopic dorsal capsuloplasty. J Wrist Surg. 2013;2:160–7.
7. Viegas SF, Yamaguchi S, Boyd NL, Patterson RM. The dorsal ligaments of the wrist: anatomy, mechanical properties and function. J Hand Surg Am. 1999;24(3):456–68.
8. Van Overstraeten L, Camus EJ, Wahegaonkar A, et al. Anatomical description of the dorsal capsulo-scapholunate septum (DCSS)-arthroscopic staging of scapholunate instability after DCSS sectioning. J Wrist Surg. 2013;2(2):149–54.

9. Mayfield JK. Patterns of injury to carpal ligaments: a spectrum. Clin Orthop Relat Res. 1984;187:36–42.
10. Messina J, Van Overstraeten L, Luchetti R, Fairplay T, Mathoulin L. The EWAS classification of scapholunate tears: an anatomical arthroscopic study. J Wrist Surg. 2013;2:105–9.
11. Linscheid RL, Dobyns JH, Beabout JW, Bryan RS. Traumatic instability of the wrist: diagnosis, classification, and pathomechanics. J Bone Joint Surg Am. 1972;54(8):1612–32.
12. Garcia-Elias M, Berger RA, Hori E, et al. Definition of carpal instability: anatomy and biomechanics committee of the international federation of societies for surgery of the hand. J Hand Surg [Am]. 1999;24(4):866–7.
13. Cerezal L, de Dios B-MJ, Canga A, et al. MR and CT arthrography of the wrist. Semin Musculoskelet Radiol. 2012;16(1):27–41.
14. Schmitt R, Froehner S, Coblenz G, Christopoulos G. Carpal instability. Eur Radiol. 2006;16(10):2161–78.
15. Watson HK, Weinzweig J, Zeppieri J. The natural progression of scaphoid instability. Hand Clin. 1997;1997(13):39–49.
16. Haisman JM, Bush M, Wolffe S. Wrist arthroscopy: standard portals and arthroscopic anatomy. J Am Soc Surg Hand. 2005;5(3):175–81.
17. Shin A. Arthroscopic anatomy of the wrist. In: Cooney WP, editor. The wrist. 2nd ed. Philadelphia: LWW; 2010. p. 253–70.
18. Geissler WB, Freeland AE, Savoie FH, McIntyre LW, Whipple TL. Intracarpal soft-tissue lesions associated with an intra-articular fracture of the distal end of the radius. J Bone Joint Surg Am. 1996;78(3):357–65.
19. Geissler WB. Arthroscopic management of scapholunate instability. J Wrist Surg. 2013;2:129–35.
20. Messina JC, Dreant N, Luchetti R, Lindau T, Mathoulin C. Scapholunate tears: a new arthroscopic classification. Chir Main. 2009;28(6):339–44.
21. Moser T, Khoury V, Harris PG, Bureau NJ, Cardinal E, Dosch JC. MDCT arthrography or MR arthrography for imaging the wrist joint? Semin Musculoskelet Radiol. 2009;13(1):39–54.
22. De Smet L. Pitfalls in wrist arthroscopy. Acta Orthop Belg. 2002;68(4):325–9.
23. Zanetti M, Gilula LA, Jacob HA, Hodler J. Palmar tilt of the distal radius: influence of off-lateral projection initial observations. Radiology. 2001;220(3):594–600.
24. Khoury V, Harris PG, Cardinal E. Cross-sectional imaging of internal derangement of the wrist with arthroscopic correlation. Semin Musculoskelet Radiol. 2007;11(1):36–47.
25. Gilula LA. Carpal injuries: analytic approach and case exercises. Am J Roentgenol. 1979;133(3):503–17.
26. Linn MR, Mann FA, Gilula LA. Imaging the symptomatic wrist. Orthop Clin N Am. 1990;21(3):515–43.
27. Gelberman RH, Cooney 3rd WP, Szabo RM. Carpal instability. Instr Course Lect. 2001;50:123–34.
28. Tanaka T, Ogino S, Yoshioka H. Ligamentous injuries of the wrist. Semin Musculoskelet Radiol. 2008;12(4):359–77.
29. Manaster BJ. Digital wrist arthrography: precision in determining the site of radiocarpal-midcarpal communication. Am J Roentgenol. 1986;147(3):563–6.
30. Moser T, Dosch JC, Moussaoui A, Buy X, Gangi A, Dietemann JL. Multidetector CT arthrography of the wrist joint: how to do it. Radiographics. 2008;28(3):787–800.
31. Bille B, Harley B, Cohen H. A comparison of CT arthrography of the wrist to findings during wrist arthroscopy. J Hand Surg [Am]. 2007;32(6):834–41.
32. Lee RK, Ng AW, Tong CS, et al. Intrinsic ligament and triangular fibrocartilage complex tears of the wrist: comparison of MDCT arthrography, conventional 3-T MRI, and MR arthrography. Skelet Radiol. 2013;42(9):1277–85.
33. Koskinen SK, Haapamäki VV, Salo J, et al. CT arthrography of the wrist using a novel, mobile, dedicated extremity cone-beam CT (CBCT). Skelet Radiol. 2013;42(5):649–57.
34. Totterman SM, Miller R, Wasserman B, Blebea JS, Rubens DJ. Intrinsic and extrinsic carpal ligaments: evaluation by three-dimensional Fourier transform MR imaging. Am J Roentgenol. 1993;160(1):117–23.
35. Shahabpour M, De Maeseneer M, Pouders C, et al. MR imaging of normal extrinsic wrist ligaments using thin slices with clinical and surgical correlation. Eur J Radiol. 2011;77(2):196–201.
36. Shahabpour M, Van Overstraeten L, Ceuterick P, De Maeseneer M, et al. Pathology of extrinsic ligaments: a pictorial essay. Semin Musculoskelet Radiol. 2012;16(2):115–28.
37. Jung JY, Yoon YC, Jung JY, Choe BK. Qualitative and quantitative assessment of wrist MRI at 3.0T: comparison between isotropic 3D turbo spin echo and isotropic 3D fast field echo and 2D turbo spin echo. Acta Radiol. 2013;54(3):284–91.
38. Lenk S, Ludescher B, Martirosan P, et al. 3.0 T high-resolution MR imaging of carpal ligaments and TFCC. RöFo. 2004;176:664–7.
39. Spaans A, Van Minnen P, Prins HJ, Korteweg MA, Schuurman A. The value of 3.0-tesla MRI in diagnosing scapholunate ligament injury. J Wrist Surg. 2013;2:69–72.
40. Mak WH, Szabo RM, Myo GK. Assessment of volar radiocarpal ligaments: MR arthrographic and arthroscopic correlation. AJR Am J Roentgenol. 2012;198(2):423–7.
41. Haims AH, Schweitzer ME, Morrison WB, et al. Internal derangement of the wrist: indirect MR arthrography versus unenhanced MR imaging. Radiology. 2003;227(3):701–7.
42. Moser T, Dosch JC, Moussaoui A, Dietemann JL. Wrist ligament tears: evaluation of MRI and combined MDCT and MR arthrography. AJR Am J Roentgenol. 2007;188(5):1278–86.
43. Taneja AK, Bredella MA, Chang CY, Joseph Simeone F, Kattapuram SV, Torriani M. Extrinsic wrist ligaments: prevalence of injury by magnetic resonance imaging and association with intrinsic ligament tears. J Comput Assist Tomogr. 2013;37(5):783–9.
44. Smith DK. MR imaging of normal and injured wrist ligaments. Magn Reson Imaging Clin N Am. 1995;3:229–48.
45. Feipel V. Anatomy of the carpal ligaments. In: Camus E, Van Overstraeten L, editors. Carpal ligament surgery, before arthritis. Paris: Springer; 2013. p. 3–18.
46. Chhabra A, Soldatos T, Thawait GK, et al. Current perspectives on the advantages of 3-T MR imaging of the wrist. Radiographics. 2012;32(3):879–96.
47. Lee RK, Griffith JF, Ng AW, Wong CW. Imaging of radial wrist pain, I: imaging modalities and anatomy. Skelet Radiol. 2014;43(6):713–24.
48. Totterman SM, Miller RJ. Scapholunate ligament: normal MR appearance on three-dimensional gradient-recalled-echo images. Radiology. 1996;200(1):237–41.
49. Burns JE, Tanaka T, Ueno T, Nakamura T, Yoshioka H. Pitfalls that may mimic injuries of the triangular fibrocartilage and proximal intrinsic wrist ligaments at MR imaging. Radiographics. 2011;31(1):63–78.
50. Sennwald GR, Zdravkovic V, Oberlin C. The anatomy of the palmar scaphotriquetral ligament. J Hand Surg (Br). 1994;76:147–9.
51. Theumann NH, Pfirrmann CW, Antonio GE, et al. Extrinsic carpal ligaments: normal MR arthrographic appearance in cadavers. Radiology. 2003;226(1):171–9.
52. Camus E. Carpal biomechanics: application to ligamentous injuries. In: Camus E, Van Overstraeten L, editors. Carpal ligament surgery, before arthritis. Paris: Springer; 2013. p. 19–38.
53. Drewniany JJ, Palmer AK, Flatt AE. The scaphotrapezial ligament complex: an anatomic and biomechanical study. J Hand Surg [Am]. 1985;10(4):492–8.
54. Holveck A, Wolfram-Gabel R, Dosch JC, et al. Scaphotrapezial ligament: normal arthro-CT and arthro-MRI appearance with

anatomical and clinical correlation. Surg Radiol Anat. 2011;33(6): 473–80.
55. Masquelet AC, Strube F, Nordin JY, et al. The isolated scapho-trapezio-trapezoid ligament injury: diagnosis and surgical treatment in four cases. J Hand Surg (Br). 1993;18:730–5.
56. Brown RR, Fliszar E, Cotten A, Trudell D, Resnick D. Extrinsic and intrinsic ligaments of the wrist: normal and pathologic anatomy at MR arthrography with three-compartment enhancement. Radiographics. 1998;18(3):667–74.
57. Short WH, Werner FW, Green JK, Masaoka S. Biomechanical evaluation of ligamentous stabilizers of the scaphoid and lunate: part II. J Hand Surg. 2005;30:24–34.
58. Rominger MB, Bernreuter WK, Kenney PJ, Lee DH. MR imaging of anatomy and tears of wrist ligaments. Radiographics. 1993;13(6):1233–46.
59. Taleisnik J. The ligaments of the wrist. J Hand Surg [Am]. 1976;1(2):110–8.
60. Roulot E. In: LeViet D, Rodineau J, Drapé JL, Tavernier T, Railhac JJ, Godefroy D, editors. Arthroscopie du poignet: intérêt diagnostique et thérapeutique dans imagerie du poignet et de la main. Paris: Sauramps Médical; 2001.
61. Reicher MA. Normal wrist anatomy, biomechanics, basic imaging protocol, and normal multiplanar MRI of the wrist. In: Reicher MA, editor. MRI of the wrist and hand. New York: Raven; 1990. p. 17–48.
62. Berger RA. The anatomy of the ligaments of the wrist and distal radioulnar joints. Clin Orthop Relat Res. 2001;383:32–40.
63. Berger RA, Landsmeer JMF. The palmar radiocarpal ligaments: a study of adult and fetal human wrist joints. J Hand Surg [Am]. 1990;15(6):847–54.
64. Zlatkin MB, Chao PC, Osterman AL, Schnall MD, Dalinka MK, Kressel HY. Chronic wrist pain: evaluation with high resolution MR imaging. Radiology. 1989;173:723–9.